

RESEARCH ARTICLE

# Exportin-T promotes tumor proliferation and invasion in hepatocellular carcinoma

Jianwei Lin<sup>1,2</sup> | Yuchen Hou<sup>1</sup>  | Shanzhou Huang<sup>1</sup> | Ziming Wang<sup>3</sup> |  
Chengjun Sun<sup>1</sup> | Zekang Wang<sup>1</sup> | Xiaoshun He<sup>1</sup> | Nga Lei Tam<sup>4</sup> |  
Chenglin Wu<sup>1</sup> | Linwei Wu<sup>1</sup>

<sup>1</sup>Department of Organ Transplantation, The First Affiliated Hospital of Sun Yat-Sen University, Guangzhou, China

<sup>2</sup>Department of Organ Transplantation, Shenzhen Third People's Hospital, Shenzhen, China

<sup>3</sup>Department of Biliary and Pancreatic Surgery, The First Affiliated Hospital of Sun Yat-sen University, Guangzhou, China

<sup>4</sup>Department of General Surgery, The Seventh Affiliated Hospital of Sun Yat-sen University, Shenzhen, China

## Correspondence

Nga Lei Tam, Department of General Surgery,  
The Seventh Affiliated Hospital of Sun Yat-sen  
University, Shenzhen 518107, China.  
Email: ngalei@gmail.com

Chenglin Wu and Linwei Wu, Department of  
Organ Transplantation, The First Affiliated  
Hospital of Sun Yat-Sen University, 58  
Zhongshan Er Road, Guangzhou 510080, China.  
Email: chenglin0311@163.com (C.W.);  
lw97002@163.com (L.W.)

## Funding information

The Nature Science Foundation of Guangdong  
Province, China, Grant numbers:  
2016A030313242, 2017A030313825; the  
National Nature Foundation of China,  
Grant numbers: 81670592, 81601391; The  
Medical Scientific Research Foundation of  
Guangdong Province, China, Grant number:  
A2016033; The Science and Technology  
Program of Guangzhou, China, Grant number:  
201804020075; the Ke Lin programme  
foundation for youth talents, Grant number:  
y50181; The Fundamental Research Funds for  
the Central Universities, Grant number:  
17ykjc9; Sanming Project of Medicine in  
Shenzhen, China, Grant number:  
SZSM201612075; Shenzhen Healthcare  
Research Project, Grant number: SZBC2017020

Exportin-T (XPOT) belongs to the RAN-GTPase exportin family that mediates export of tRNA from the nucleus to the cytoplasm. Up-regulation of XPOT indicates poor prognosis in breast cancer patients. However, the correlation between XPOT and hepatocellular carcinoma (HCC) remains unclear. Here, we found that high expression of XPOT in HCC indicated worse prognosis via bioinformatics analysis. Consistently, immunohistochemical staining of 95 pairs of tumors and adjacent normal liver tissues (ANLT) also showed up-regulation of XPOT. Small interfering (si) RNA transfection was used to down-regulate XPOT in HepG2 and 7721 cell lines. Cell Counting Kit-8 (CCK8) assays were performed to analyze cell proliferation. Cell migration and invasion were measured by scratch wound healing assays and migration assays. Subcutaneous xenograft models were used to explore the role of XPOT in tumor formation in vivo. Down-regulation of XPOT significantly inhibited tumor proliferation and invasion in vitro and vivo. Gene set enrichment analysis (GSEA) results indicated that XPOT may affect tumor progression through cell cycle and ubiquitin-mediated proteolysis. Furthermore, knockdown of XPOT caused a block in G0/G1 phase as evidenced by down-regulation of cyclin-dependent kinase 1 (CDK1), cyclin-dependent kinase 2 (CDK2), cyclin-dependent kinase 4 (CDK4), CyclinA1 (CCNA1), CyclinB1 (CCNB1), CyclinB2 (CCNB2), and CyclinE2 (CCNE2) in HCC cells. In conclusion, our findings indicate that XPOT could serve as a novel biomarker for prognoses and a potential therapeutic target for patients with HCC.

**Abbreviations:** ANLT, adjacent normal liver tissue; ATCC, American Type Culture Collection; CCN, cyclin; CDK, cyclin-dependent kinase; CCK-8, Cell Counting Kit-8; FC, fold change; FFPE, formalin-fixed, paraffin-embedded; GEO, Gene Expression Omnibus; GLM, generalized linear models; GSEA, Gene Set Enrichment Analysis; HCC, Hepatocellular Carcinoma; OS, overall survival; qRT-PCR, quantitative real-time polymerase chain reaction; siRNA, small interfering; SKP2, S-phase kinase-associated protein 2; TCGA, The Cancer Genome Atlas; tRNA, Transfer Ribonucleic Acid; UPS, ubiquitin-proteasome system; XPOT, Exportin-T.

Jianwei Lin, Yuchen Hou, and Shanzhou Huang contributed equally to this work.

This is an open access article under the terms of the Creative Commons Attribution-NonCommercial License, which permits use, distribution and reproduction in any medium, provided the original work is properly cited and is not used for commercial purposes.

© 2018 The Authors. *Molecular Carcinogenesis* Published by Wiley Periodicals, Inc.

## KEYWORDS

bio-marker, cell cycle, exportin-T (XPOT), hepatocellular carcinoma (HCC), ubiquitin mediated proteolysis

## 1 | INTRODUCTION

Hepatocellular carcinoma (HCC) is the one of the leading causes of cancer death worldwide.<sup>1</sup> The incidence of HCC is increasing due to the prevalence of obesity and diabetes mellitus.<sup>2</sup> A high frequency of tumor recurrence and metastasis leads to poor prognosis.<sup>3,4</sup> Although some progress has been made in the study of HCC in recent years,<sup>5-7</sup> existing therapeutic methods have limited effects on advanced HCC patients. The underlying mechanism of HCC remains unclear. Therefore, further exploration of the mechanism of HCC progression will contribute to the development of new therapeutic targets.

Exportin-T (XPOT) is a member of the importin (karyopherin)  $\beta$  family, which is characterized as a nuclear export receptor for tRNAs.<sup>8</sup> XPOT can translocate tRNAs from the nucleus to the cytoplasm by forming a ternary transport complex with Ran-GTP and newly synthesized tRNAs.<sup>9</sup> XPOT plays a prominent role in coordination between the protein translation and the nuclear tRNA processing and transport machineries.<sup>10</sup> Previous studies have shown that XPOT can promote tumor progression in various cancers. XPOT was found to be up-regulated in malignant pleural mesothelioma.<sup>11</sup> Elevated XPOT contributes to chromosome instability and worsen breast cancer patient prognosis.<sup>12</sup> Decreased expression of XPOT was related to inhibition of cell proliferation in human promyelocytic leukemia HL-60 cells.<sup>13</sup> However, whether XPOT functions in tumor progression has still not been studied. Here, we found elevated expression of XPOT in HCC and further explored the role of XPOT in tumor proliferation and invasion for the first time.

In our study, we found that XPOT was significantly up-regulated in TCGA datasets, GEO (GSE6764, GSE14520, GSE36376, GSE45436, and GSE62232) and HCC patients, indicating poor prognosis. Down-regulation of XPOT inhibited tumor proliferation and invasion *in vitro* and *in vivo*. Gene sets enrichment analysis (GSEA) results indicated that XPOT was closely related to cell cycle and ubiquitin-mediated proteolysis. Mechanistically, knockdown of XPOT significantly decreased the expression of cyclin-dependent kinase 1 (CDK1), cyclin-dependent kinase 2 (CDK2), cyclin-dependent kinase 2 (CDK4), CyclinA1 (CCNA1), CyclinB1 (CCNB1), CyclinB2 (CCNB2), and CyclinE2 (CCNE2) in HCC cells. Herein, we demonstrated that XPOT promotes tumor proliferation and invasion in HCC.

## 2 | MATERIALS AND METHODS

### 2.1 | Patients' information and tissue samples

All tissues samples were obtained from HCC patients who underwent a hepatectomy at the First Affiliated Hospital of Sun Yat-sen University (Guangzhou, China) between July 2013 and December 2014. None of them received radiotherapy or preoperative chemotherapy before

surgery. All patients were followed up until December 2017. The detailed information on the clinical characteristics of all patients is shown in Table 1. All specimens were handled and made anonymous according to the ethical and legal standards. All fresh tumor tissue specimens were snap-frozen in liquid nitrogen and stored at  $-80^{\circ}\text{C}$  immediately after resection. Overall survival (OS) was defined as the period between surgery and death or the last contact. Disease-free survival (DFS) was defined as the period between surgery and any form of tumor recurrence.

### 2.2 | High-throughput data processing

The expression data for HCC were obtained from TCGA (<http://gdc.cancer.gov/>) and GEO GSE6764, GSE14520, GSE36376, GSE45436 and GSE62232 (<http://www.ncbi.nlm.nih.gov/geo>). All data were log2 transformed, and the results were analyzed using edgeR and GraphPad Prism 7 software. The edgeR package that we used was based on negative binomial distributions, empirical Bayes estimation, exact tests, generalized linear models (GLM) and quasi-likelihood tests. A logFC (fold change)  $\geq 1.0$  or logFC  $\leq -1.0$  associated with a  $P < 0.05$  was selected as statistically significant for the genes.

### 2.3 | Immunohistochemical staining and antibodies

Tissue specimens from 95 cases of HCC fixed in formalin and embedded in paraffin were used for XPOT immunohistochemistry. XPOT antibodies for immunohistochemistry staining were obtained from Bioss (bs-14673R). After deparaffinization, hydration and blocking, the specimens were mixed with primary anti-XPOT goat polyclonal antibody and then incubated overnight at  $4^{\circ}\text{C}$  (dilution ratio 1:1000). Finally, all sections were assessed by comparison of staining between each HCC and normal specimen under a microscope. The total scores were determined with two scores: the positive cell score and staining intensity score. The staining intensity score is as follows: 0: no staining; 1: slightly yellower than the background; 2: yellow brown; 3: brown. The positive cell score is as follows: 0: 0 ~ 5%; 1: 6 ~ 25%; 2: 26 ~ 50%; 3: 51 ~ 75%; 4: >75%. The immunohistochemistry total score was calculated as the positive cell score  $\times$  the staining intensity score. The total score was classified by four levels: 0 for negative (-); 1-4 for the weakly positive (+); 5-8 for positive (++); and 9-12 for strongly positive (+++).

### 2.4 | RNA extraction and quantitative real-time polymerase chain reaction (qRT-PCR)

Total RNA was extracted with TRIzol reagent (Invitrogen, NY) according to the manufacturer's instructions. qRT-PCR was performed using the SYBR Green detection RT-PCR system (TaKaRa, Japan) with the following primers for XPOT: sense primer: GGATGAACAGGCTCTATTAGGGC;

**TABLE 1** Correlation between XPOT expressions with clinicopathological characteristics of HCC

Clinicopathological variables	N	XPOT expression		P-value
		Low (34)	High (61)	
<b>Sex</b>				
Male	81	22	59	1.000
Female	14	4	10	
<b>Age, years</b>				
<50	48	12	36	0.650
≥50	47	14	33	
<b>AFP, ng/L</b>				
<200	50	18	32	0.065
≥200	45	8	37	
<b>HBsAg</b>				
Negative	41	9	32	0.358
Positive	54	17	37	
<b>Tumor size, cm</b>				
≤5	49	18	31	<b>0.041</b>
>5	46	8	38	
<b>Tumor nodule number</b>				
Solitary	58	19	39	0.163
Multiple (≥2)	37	7	30	
<b>Cancer embolus</b>				
Absence	65	22	43	<b>0.048</b>
Presence	30	4	26	
<b>TNM stage</b>				
Early (I & II)	51	20	31	<b>0.006</b>
Late (III & IV)	44	6	38	
<b>Differentiation grade</b>				
Well	64	24	40	<b>0.001</b>
Poor	31	2	29	

AFP, alpha fetoprotein; HBsAg, hepatitis B surface antigen. Bold values represent *P* values which are smaller than 0.05. In this table, high expression of XPOT is closely related with tumor size (>5 cm), cancer embolus, late TNM stage, and poor differentiation grade.

anti-sense primer: TGCAGCCATGATATGAGCGTC; and GAPDH (forward primer: TGTGGGCATCAATGGATTGG and reverse primer: ACACCATGTATTCCGGGTCAAT) (Servicebio Technology, Wuhan, China). GAPDH was used as the reference control. The relative mRNA expression levels were quantified using the  $2^{-\Delta\Delta C_t}$  method. All qRT-PCR experiments were performed in triplicate.

## 2.5 | Cell culture and transfection

Human HCC cell lines (HepG2 and SMCC-7721) were obtained from the American Type Culture Collection (ATCC, Manassas, VA) and maintained in DMEM supplemented with 10% fetal bovine serum with antibiotics (penicillin and streptomycin) at 37°C in a humidified 5% CO<sub>2</sub>

atmosphere. To inhibit XPOT expression, we transfected three small interfering RNAs (siRNAs) targeting the XPOT coding sequence. The siRNA sequences were as follows:

1. GCTCAAAGATTGTGAAGCA
2. GAATCCTCATGGCTATTGA
3. GGACAGTCATTGATAGTTA

The XPOT knockdown vector was constructed by Shanghai Generay Biotech Co., Ltd. For packaging of the construct, 293TN cells were transfected with sh-XPOT/NC by pPACKH1 Packaging Plasmid Mix. The virus particles were collected with Lenti-Concentin Virus Precipitation Solution according to the packaging protocol of SBI after 3 days. Cells were infected with TransDux virus transduction reagent. The target sequences were as follows:

1. GAATCCTCATGGCTATTGA
2. GGACAGTCATTGATAGTTA

Positive cells were identified by puromycin screening.

## 2.6 | Western blot and antibodies

The cells were washed twice with 4°C PBS and then lysed in cold RIPA buffer with protease inhibitors. The BCA Protein Quantitation Assay (KeyGen Biotech, Nanjing, China) was used to measure the protein concentration. The total protein was transferred to a nitrocellulose membrane after denaturing by 10% SDS-PAGE. The membranes were blocked with 5% non-fat milk in Tris-buffered saline containing 0.1% Tween-20 (TBST) for 1 h at room temperature. The membranes were then incubated with the following primary antibodies overnight at 4°C (dilution ratio 1:2000). The membranes were washed three times with TBST and then incubated with secondary antibodies (anti-rabbit IgG or anti-mouse IgG) for 1 h at room temperature. The membranes were washed three times with TBST, and then, the targeted proteins were detected by the ECL (EMD Millipore, MA, USA) method. XPOT, CDK1, CDK2, CDK4, CCNA1, CCNB1, CCNB2, CCNE2 antibodies for western blot were obtained from Bioss (bs-14673R), Abcam (ab133327), Abcam (ab32147), Abcam (ab108357), Abcam (ab53699), Abcam (ab32053), Abcam (18250), Abcam (40890).

## 2.7 | Cell proliferation assay

Cell Counting Kit-8 (CCK8, Dojindo, Tabaru, Japan) was used to measure cell proliferation. The cells were seeded into 96-well plates. The absorption values were measured at following time points: 24, 48, 72, and 96 h after siRNA transfection. The assays were repeated three times, and the data are shown as the mean ± SD.

## 2.8 | Flow cytometry

For the cell cycle analysis, HCC cells were harvested, fixed in 75% ethanol and stored at 4°C overnight. Then, the cells were stained with DNA Prep

(Beckman Coulter, Brea, CA), and flow cytometry was performed to detect the percentage of cells in different phases according to their DNA content.

## 2.9 | Scratch wound healing assay

HCC transfected cells were seeded into 6-well plates and then were incubated at 37°C with 5% CO<sub>2</sub> until they reached 100% confluence. Then, a 10-μL pipette was used to scratch the monolayer. After cell

fragments were washed away, the cells were cultured under normal conditions. Photograph were taken at 0 and 24 h. The data are shown as the relative distance between two edges.

## 2.10 | Cell invasion assay

Cell invasion was assessed by Transwell chambers. Transwell assays were performed using polyethylene terephthalate-based migration chambers

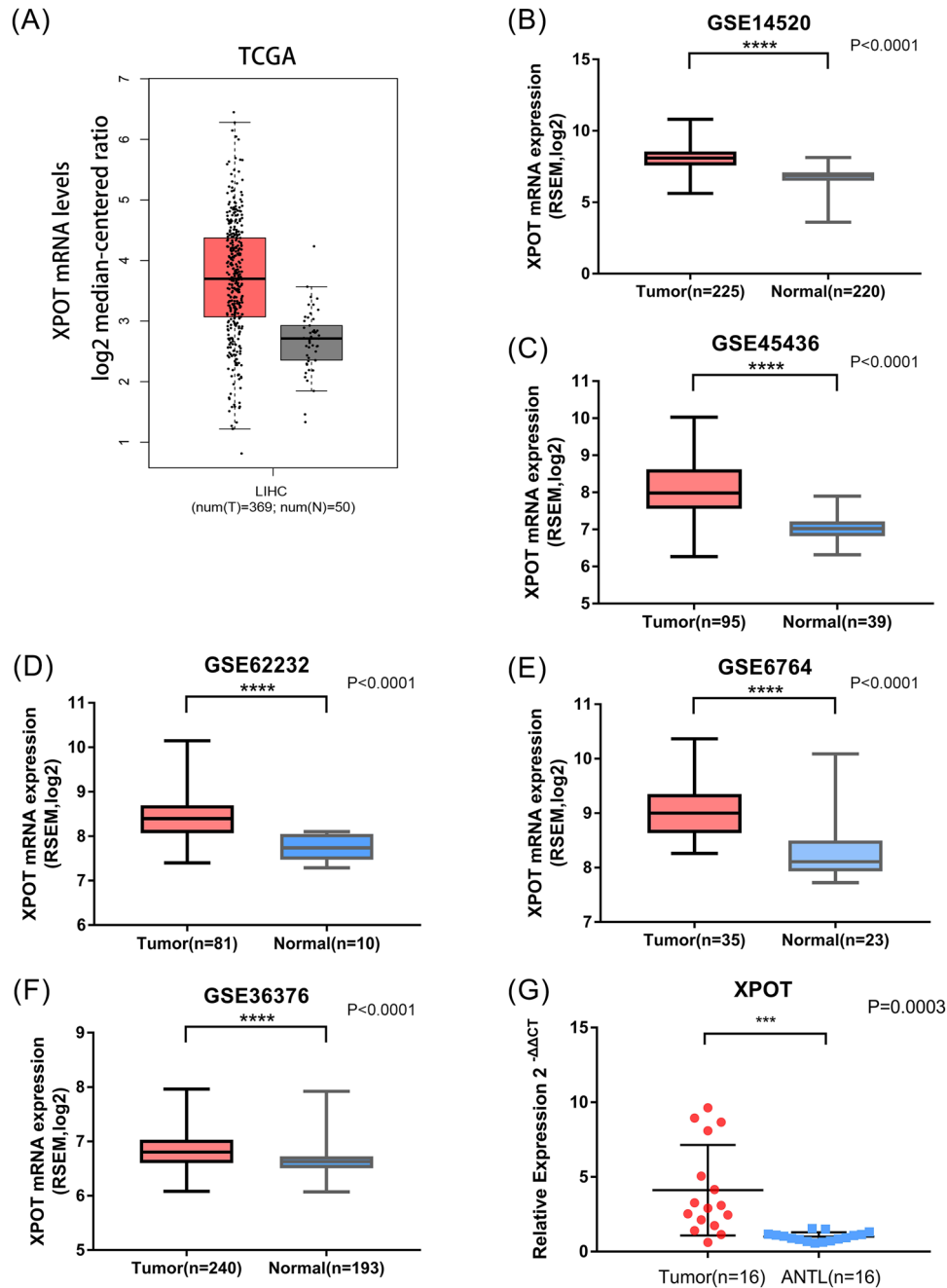


**FIGURE 1** XPO1 is upregulated in HCC tissues compared with ANLTs. XPO1 was highly expressed in HCC tissues compared with normal liver tissues according to analysis of data from TCGA (A; tumor,  $n = 369$ ; normal = 50,  $*P < 0.01$ ) and GEO (B-F; GSE14520, tumor,  $n = 225$ ; normal,  $n = 220$ ,  $****P < 0.0001$ ; GSE45436, tumor,  $n = 95$ ; normal,  $n = 39$ ,  $****P < 0.0001$ ; GSE62232, tumor,  $n = 81$ ; normal,  $n = 10$ ,  $****P < 0.0001$ ; GSE6764, tumor,  $n = 35$ ; normal,  $n = 23$ ,  $****P < 0.0001$ ; GSE36376, tumor,  $n = 240$ ; normal,  $n = 193$ ,  $****P < 0.0001$ ). (H) Real-time PCR analysis of XPO1 expression in 16 pairs of HCC specimens and corresponding ANLTs ( $***P = 0.0003$ ). All  $*P < 0.05$ ,  $**P < 0.01$ ,  $***P < 0.001$ ,  $****P < 0.0001$ . [Color figure can be viewed at [wileyonlinelibrary.com](http://wileyonlinelibrary.com)]

and BD BioCoat Matrigel Invasion Chambers (Becton Dickinson Labware). Cells in serum-free media were distributed into the inserts. Equal amounts of growth media were placed into the wells. After overnight culture, the chamber membrane was stained with 50% methanol blue/ethanol overnight. The data are shown as the mean  $\pm$  SD.

## 2.11 | Animal experiments

Animal experiments were performed according to the protocol filed with the Guidance of Institutional Animal Care and Use Committee

(IACUC) of Sun Yat-Sen University and with the approval of the Institutional Review Board of Sun Yat-Sen University. To establish subcutaneous xenograft models,  $2 \times 10^6$  HepG2 cells were subcutaneously injected into the right flank of nude mice. The tumor volume was measured every 7 days by means of a caliper and calculated as  $(\text{length} \times \text{width}^2)/2$ . Twenty-eight days after implantation, the mice were euthanized by cervical dislocation and the tumor xenografts were excised, fixed, weighted, photographed and stored.

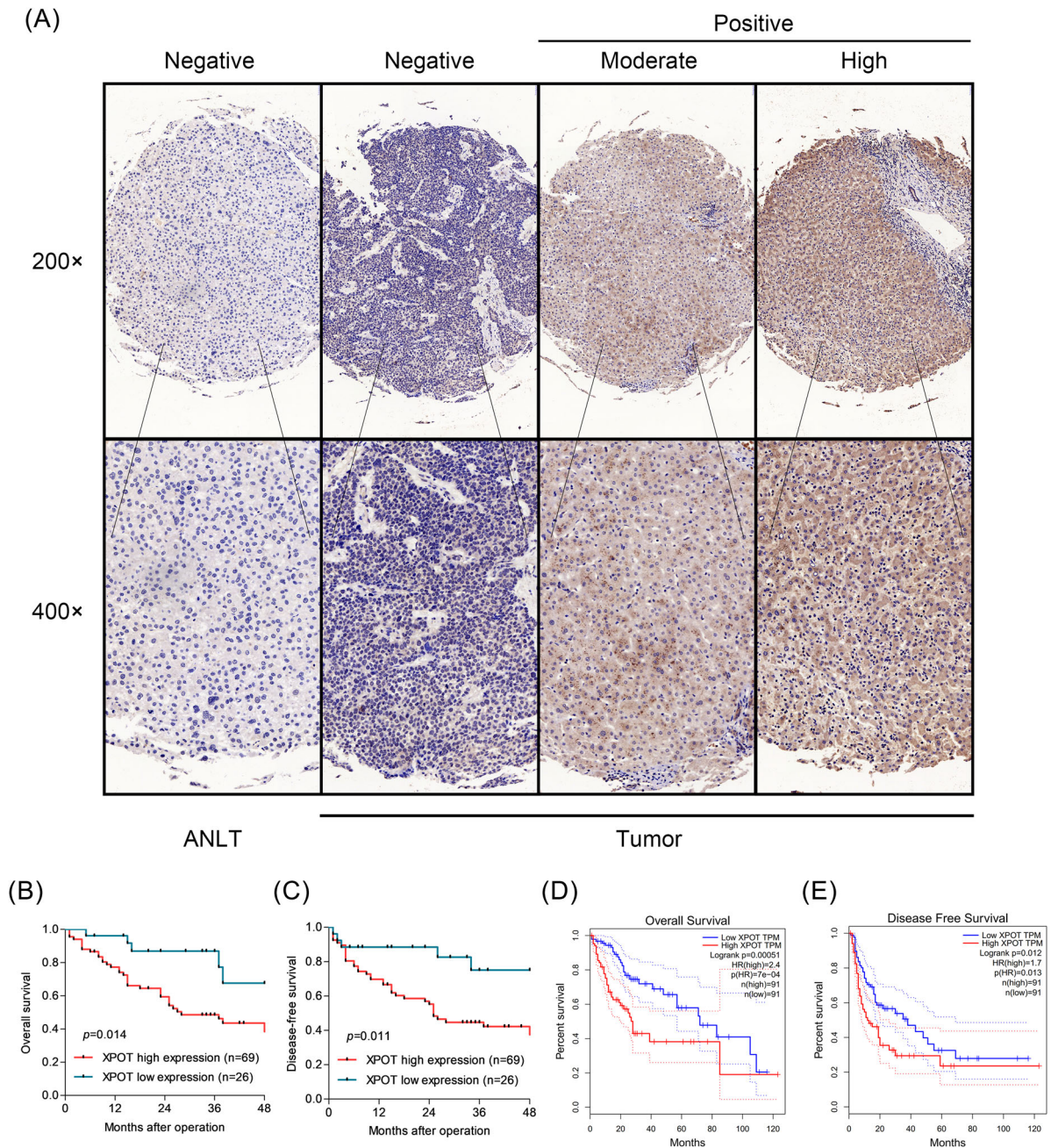


**FIGURE 2** (A) XPOT expression is correlated with clinicopathological features and poor prognosis. Immunohistochemical staining showed low XPOT expression in normal liver tissues and HCC tissues. The scales bars indicate 50 and 20  $\mu\text{m}$ . (B-C) Overall survival and disease-free survival curves for HCC patient groups. (D-E) Overall survival and disease-free survival analysis of TCGA. All  $*P < 0.05$ ,  $**P < 0.01$ ,  $***P < 0.001$ ,  $****P < 0.0001$ . [Color figure can be viewed at [wileyonlinelibrary.com](http://wileyonlinelibrary.com)]

**TABLE 2** Univariate and multivariate Cox regression analysis of risk factors associated with overall survival

Variables	Univariate analysis			Multivariate analysis		
	HR	95%CI	P-value	HR	95%CI	P-value
XPOT expression (High vs Low)	3.17	1.24-8.09	<b>0.016</b>	2.39	1.02-6.22	<b>0.044</b>
Sex (Male vs Female)	2.89	0.89-9.40	0.08			
Age ( $\geq 50$ vs $< 50$ )	1.09	0.59-2.00	0.79			
HBsAg (Positive vs Negative)	2.58	1.38-4.83	<b>&lt;0.01</b>	1.73	0.90-3.33	0.10
AFP ( $\geq 200$ ng/mL vs $< 200$ ng/mL)	2.44	1.30-4.58	<b>0.01</b>	1.70	0.87-3.32	0.12
Tumor size ( $> 5$ cm vs $\leq 5$ cm)	1.44	0.77-2.71	0.26			
Tumor nodule number (Multiple vs Single)	1.5	0.81-2.75	0.20			
Cancer embolus (Presence vs Absence)	2.39	1.28-4.43	<b>0.01</b>	1.62	0.81-3.24	0.18
TNM stage (Late vs Early)	2.58	1.38-4.83	<b>&lt;0.01</b>	0.14	0.83-3.74	0.14
Differentiation grade (Poor vs Well)	1.37	0.98-1.86	0.05			

AFP, alpha fetoprotein; HBsAg, hepatitis B surface antigen. Bold values represent P values which are smaller than 0.05. In this table, univariate cox regression analysis showed that overall survival rate is correlated with XPOT expression, HBV infection, AFP, cancer embolus, and TNM stage. Multivariate cox regression analysis suggested that XPOT can serve as an independent risk factor for overall survival in HCC patients.

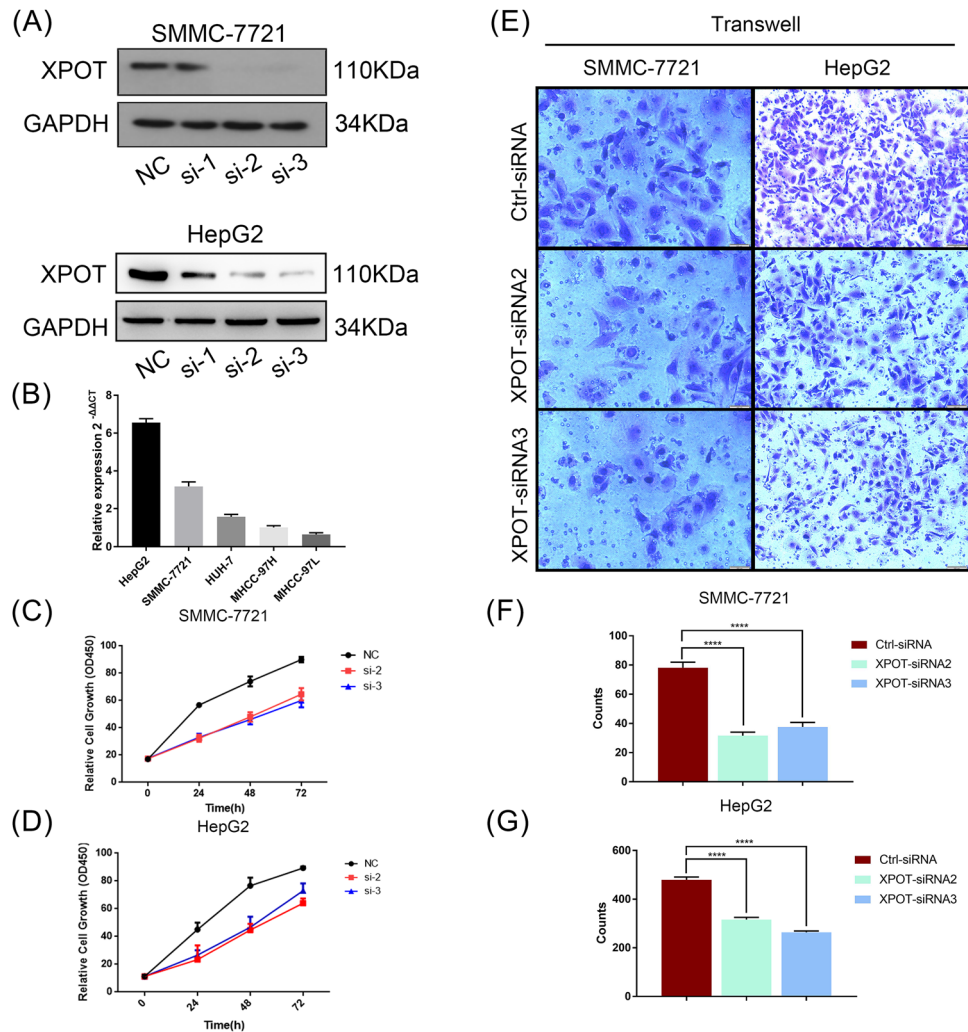


**FIGURE 3** Inhibition of XPOT affects cell proliferation and invasion. (A) Down-regulation of XPOT expression using different siRNA sequences. (B) Expression levels of XPOT in HCC cell lines. (C)-(D) Effects of XPOT silencing on cell proliferation were evaluated with CCK8 assays in transfected SMMC-7721 and HepG2 cells. (E-G) Down-regulation of XPOT inhibited the invasive ability of HepG2 and SMMC-7721 cells. All  $*P < 0.05$ ,  $**P < 0.01$ ,  $***P < 0.001$ ,  $****P < 0.0001$ . [Color figure can be viewed at [wileyonlinelibrary.com](http://wileyonlinelibrary.com)]

## 2.12 | GSEA

GSEA was performed to identify gene sets and pathways associated with XPOT using the data obtained from TCGA. GSEA is supported by the Broad Institute Website (<http://software.broadinstitute.org/gsea/index.jsp>).<sup>14</sup> Each gene in the list was weighted by its log fold change in expression.

## 2.13 | Statistical analysis

All data analyses were performed with edgeR. Pearson correlation coefficients were used to assess patient specimens. The Cox proportional hazards model was used to calculate survival rates. Survival curves were calculated by the Kaplan-Meier method. The significance of data in vivo and in vitro was determined by Student's *t*-test. All experiments were independently repeated at least three times.  $P < 0.05$  was considered statistically significant.

## 3 | RESULTS

### 3.1 | XPOT is upregulated in human HCC and correlated with poor clinical characteristics

Gene expression data and corresponding clinical information were obtained from TCGA database and GEO (GSE6764, GSE14520, GSE36376, GSE45436 and GSE62232). XPOT was elevated in all datasets, and the detailed results are summarized in Figure 1. Real-time PCR analyses of 16 pairs of fresh tumor tissues and corresponding adjacent normal liver tissues (ANLT) verified the upregulation of XPOT in HCC tissues (Figure 1G). Immunostaining results showed that the expression levels of XPOT were high in 69 of the 95 HCC cases and low in 26 (Figure 2A). The correlations between the XPOT expression and clinical characteristics of HCC patients are summarized in Table 1. The expression of XPOT was positively related to tumor size ( $P = 0.041$ ), tumor nodule number ( $P = 0.028$ ), cancer embolus ( $P = 0.048$ ) and differentiation grade ( $P = 0.001$ ). These results suggest that XPOT is

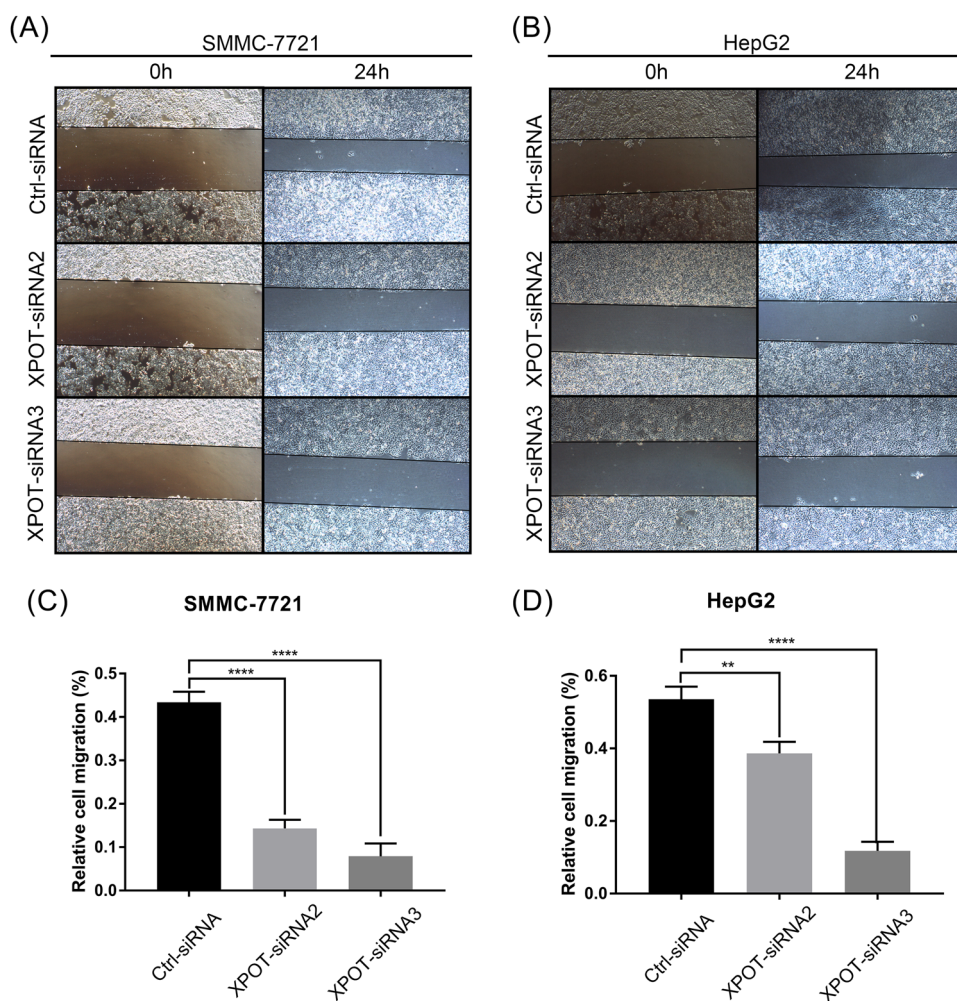


**FIGURE 4** Down-regulation of XPOT affects motility in SMMC-7721 and HepG2 cells. (A-B) Effects of XPOT on wound healing in transfected SMMC-7721 and HepG2 cells (200 $\times$ ). (C-D) The data were calculated as the relative cell migration (%) at 0 and 24 h. All  $*P < 0.05$ ,  $**P < 0.01$ ,  $***P < 0.001$ ,  $****P < 0.0001$ . [Color figure can be viewed at [wileyonlinelibrary.com](http://wileyonlinelibrary.com)]

upregulated in human HCC tissues and is positively correlated with HCC malignancy.

### 3.2 | Overexpression of XPOT predicts poor survival in patients with HCC

To determine the prognostic value of XPOT, we performed Kaplan-Meier analysis, and the results are shown in Figure 2. Overexpression of XPOT indicated inferior OS and DFS. Then, we used a Cox proportional hazard model to examine whether XPOT can serve as independent prognostic factor in 95 HCC patients in our center. The results indicated that the patients with high XPOT expression level had a poor prognosis (Figure 2). The multivariate analysis demonstrated that XPOT expression (HR 2.39, 95%CI 1.02-6.22,  $P < 0.05$ ) was an independent prognostic factor for OS (Table 2). XPOT can serve as an independent prognostic biomarker for HCC patients.

### 3.3 | Altered XPOT expression affects cell proliferation

We examined the expression of XPOT in 5 HCC cell lines and found the higher expression of XPOT in HepG2 and SMMC-7721

(Figure 3B). To investigate the function of XPOT in HCC, we transfected the HepG2 and SMMC-7721 cell lines with three siRNAs (si-1, si-2, and si-3) targeting XPOT and control siRNA. Western blot analyses indicated that the expression of XPOT was significantly decreased in XPOT-siRNA-transfected cells compared with that of the control groups (Figure 3A). The CCK8 assay results indicated that downregulation of XPOT in both HepG2 and 7721 cell lines inhibited cell proliferation compared with that of the control groups at 24 h after transfection ( $P < 0.05$ ; Figures 3C and 3D).

### 3.4 | Down-regulation of XPOT decreases HCC cell motility

Scratch wound healing assays and invasion assays were performed to detect the effect of XPOT on cell motility. The XPOT-siRNA groups showed a lower migratory capacity than the control groups ( $P < 0.05$ ). In the invasion assay, downregulation of XPOT significantly decreased the invasive abilities of both SMMC-7721 cells ( $P < 0.05$ ) and HepG2 cells ( $P < 0.05$ ; Figures 3E-G). XPOT-siRNA cells closed the scratch wounds more slowly than control cells at 24 h in the HepG2 ( $P < 0.05$ ) and 7721 ( $P < 0.05$ ) cell lines (Figure 4). These data suggest that XPOT plays a critical role in the motility of HCC cells.

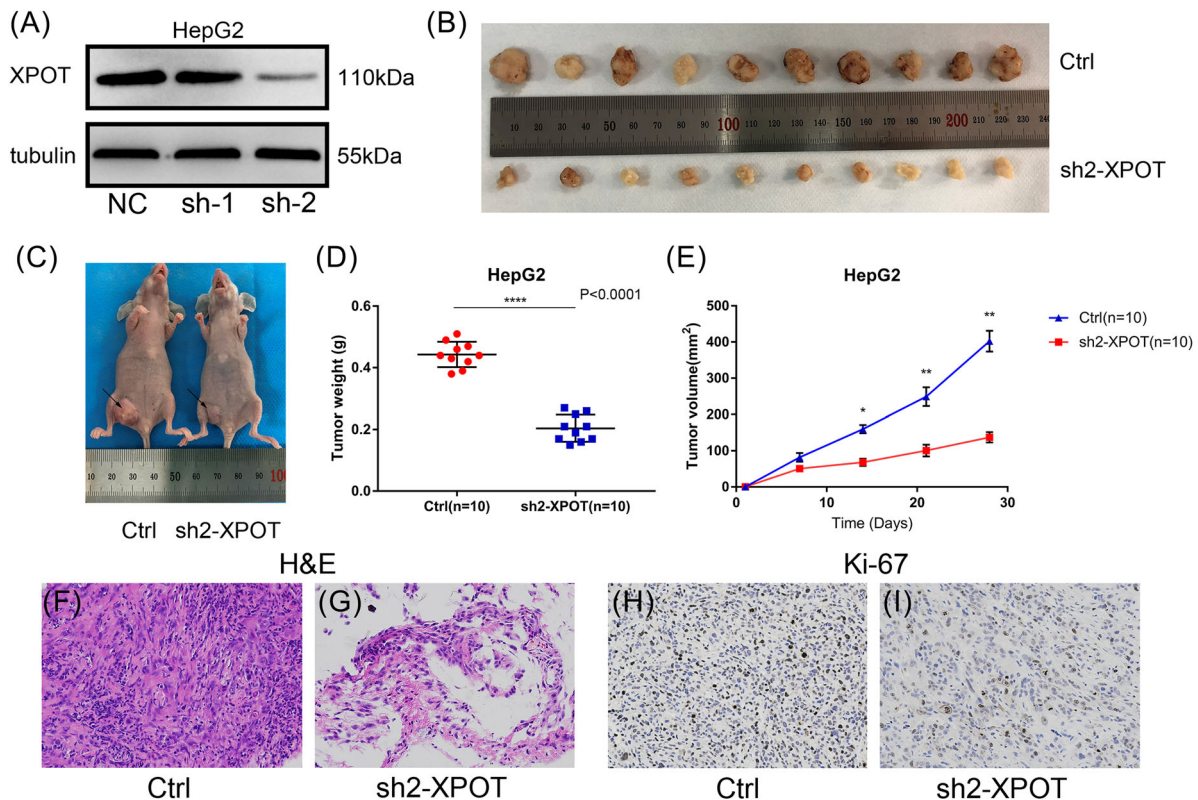


**FIGURE 5** Knockdown of XPOT impaired HCC carcinogenesis in vivo. (A) Down-regulation of XPOT expression using different shRNA. (B-C) The nude mice were sacrificed twenty-eight days after the injection and tumors from respective groups were shown. (D) Tumor weight was measured in sh-XPOT and control groups ( $****P < 0.0001$ ). (E) Tumor growth curves after the injection of HepG2 cells. Tumor volume was calculated every 7 days. (F-G) H&E staining of tumors with different treatments. (H-I) IHC staining of Ki67 in tumors with different treatments. All  $*P < 0.05$ ,  $**P < 0.01$ ,  $***P < 0.001$ ,  $****P < 0.0001$ . [Color figure can be viewed at [wileyonlinelibrary.com](http://wileyonlinelibrary.com)]

### 3.5 | The knockdown of XPOT inhibited tumor proliferation and invasion in vivo

To test whether the expression level of XPOT could affect tumor progression in vivo, we constructed XPOT stable knockdown HepG2 cell lines using lentivirus carrying shRNA (Figure 5A). XPOT knockdown cells and control cells were subcutaneous injected into BALB/c nude mice. The XPOT-deficient tumors grew more slowly than that in control group (Figures 5B-E). The mice were euthanized, and tumors were measured 28 days after the cell injection. The tumor weight at the end of

the experiment was markedly lower in the shXPOT-transfected HepG2 group ( $P < 0.0001$ ; Figure 5D). Moreover, IHC staining showed that proliferation marker gene Ki-67 was dramatically downregulated in XPOT knockdown tumors (Figures 5H and 5I). These findings indicated that the knockdown of XPOT inhibits tumorigenesis in vivo.

### 3.6 | GSEA

GSEA was conducted to investigate the mechanism of XPOT orchestrating tumor cell proliferation and invasion in

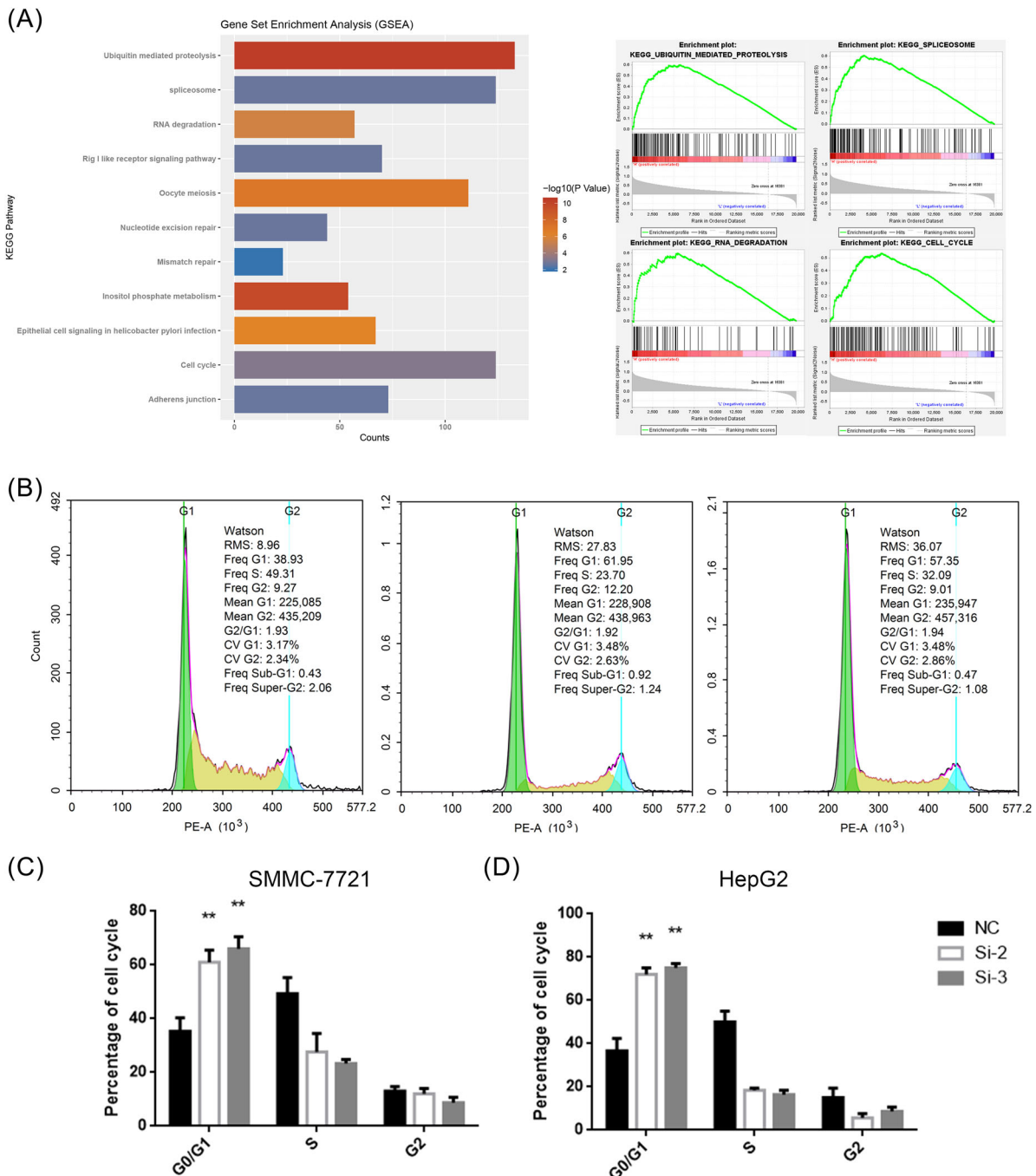


**FIGURE 6** Down-regulation of XPOT affects the cell cycle and may be related to ubiquitin-mediated proteolysis. XPOT was correlated with gene sets in ubiquitin-mediated proteolysis, RNA degradation, spliceosome and cell cycle in GSEA. (A) Inhibition of XPOT triggered G0/G1 block in the cell cycle. (B-D). All  $*P < 0.05$ ,  $**P < 0.01$ ,  $***P < 0.001$ ,  $****P < 0.0001$ . [Color figure can be viewed at wileyonlinelibrary.com]

HCC. As shown in Figure 6A, XPOT was significantly correlated with gene sets in ubiquitin-mediated proteolysis, RNA degradation, spliceosomes and cell cycle. XPOT is most likely to affect tumor progression through ubiquitin-mediated proteolysis, which had 90 related gene counts. We further performed flow cytometry to investigate the effect of XPOT the cell cycle. As shown in Figures 6B to D, the cell cycle of the XPOT-siRNA groups was blocked in G0/G1 phase ( $P < 0.05$ ).

### 3.7 | XPOT promoted HCC progression by up-regulating cyclins and CDKs

For down-regulation of XPOT led to the block in G0/G1 phase in HepG2 and SMMC-7721 cell lines, we analyzed the relationships between XPOT and cyclins and CDKs using TCGA datasets. The expression of CDK1, CDK2, CDK4, CCNA1, CCNB1, CCNB2 and CCNE2 were positively related with XPOT (Pearson correlation coefficient  $r > 0.3$ ) (Figure 7A). Western blot results showed that

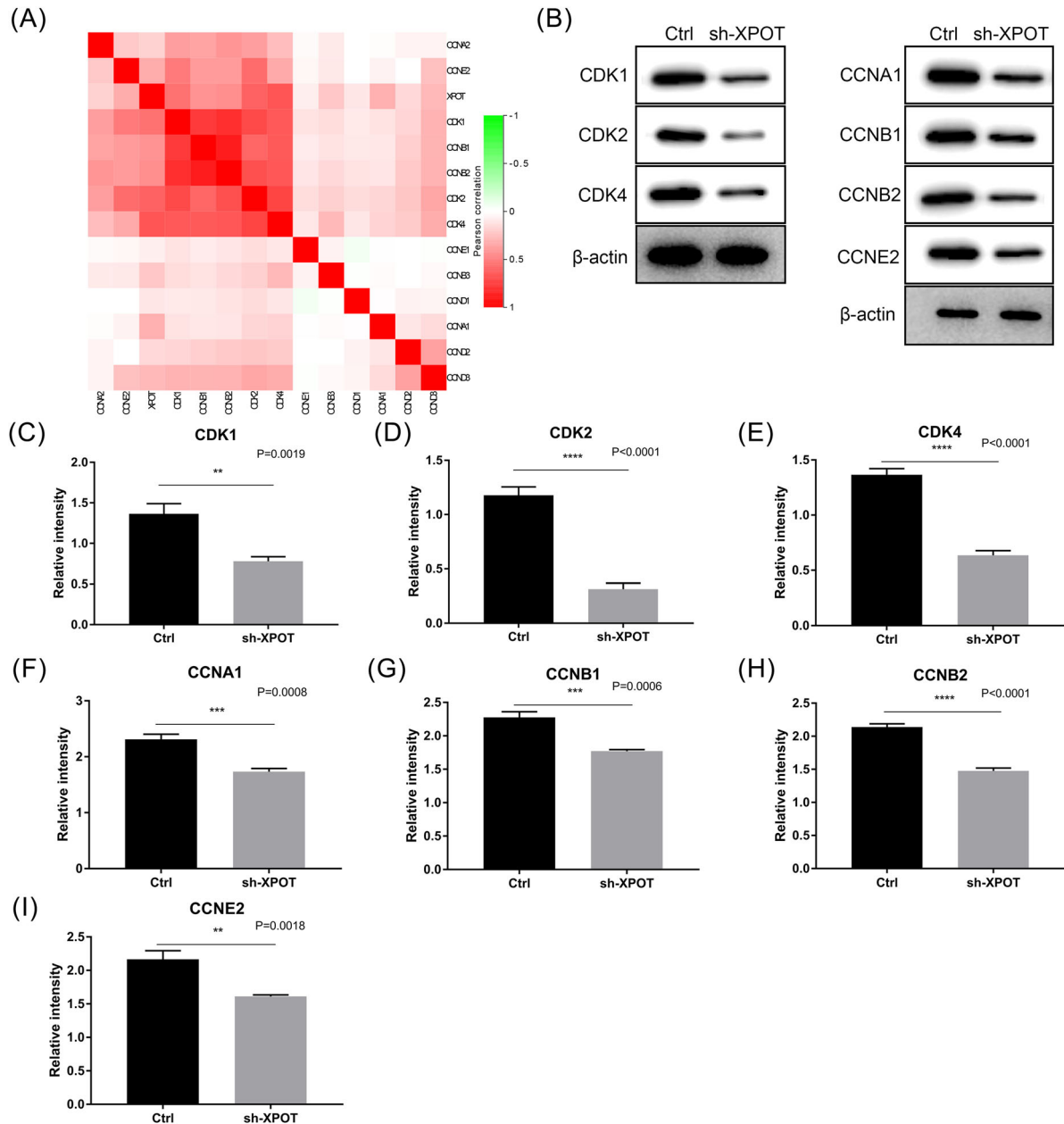


**FIGURE 7** XPOT promoted HCC progression by up-regulating cyclins and CDKs. (A) XPOT was positive correlated with CDK1, CDK2, CDK4, CCNA1, CCNB1, CCNB2 and CCNE2. (B) Knockdown of XPOT inhibited the protein expression of CDK1, CDK2, CDK4, CCNA1, CCNB1, CCNB2 and CCNE2. (C-I) Relative density of cyclins and CDKs in sh2-XPOT and control groups (CDK1,  $**P = 0.0019$ ; CDK2,  $****P < 0.0001$ ; CDK4,  $****P < 0.0001$ ; CCNA1,  $***P = 0.0008$ ; CCNB1,  $***P = 0.0006$ ; CCNB2,  $****P < 0.0001$ ; CCNE2,  $**P = 0.0018$ ). All  $*P < 0.05$ ,  $**P < 0.01$ ,  $***P < 0.001$ ,  $****P < 0.0001$ . [Color figure can be viewed at [wileyonlinelibrary.com](http://wileyonlinelibrary.com)]

CDK1, CDK2, CDK4, CCNA1, CCNB1, CCNB2 and CCNE2 were lower in sh2-XPOT treated cells (Figure 7B).

## 4 | DISCUSSION

In the present study, we found significant upregulation of XPOT in TCGA datasets, GEO, 95 pairs of clinical samples by immunohistochemical staining and 16 pairs of fresh tumor specimens by qRT-PCR. Elevated XPOT indicated poor prognosis in HCC patients. Then, we down-regulated the expression of XPOT in HCC cells. CCK8 assays Transwell assays and subcutaneous xenograft models showed that inhibition of XPOT suppressed cell proliferation and invasion in vitro and vivo. XPOT is likely to play an important role in tumor progression in HCC.

XPOT is a Ran-GTP-dependent tRNA receptor orchestrating translocation of tRNA from the nucleus to the cytoplasm in human cells.<sup>15,16</sup> XPOT binds to mature tRNAs directly by recognizing the base of the acceptor arm, the TΨC loop and correctly matured 5' and 3' ends.<sup>15,17,18</sup> The regulation of gene expression relies in part on the controlled exchange of XPOT. Emerging evidence has linked Importin  $\beta$ -like nuclear export receptors to several types of diseases, including cancers.<sup>19,20</sup> Elevated expression of XPOT is associated with cell proliferation in human promyelocytic leukemia.<sup>13</sup> Overexpression of XPOT leads to more aggressive and chromosomally unstable breast cancers.<sup>12</sup> However, the role of XPOT in HCC has not been studied before. We demonstrated that XPOT promotes cell proliferation and invasion in HCC for the first time.

How does XPOT affect tumor progression in HCC? GSEA and flow cytometry results suggested that XPOT may promote tumor progression through cell cycle. Moreover, the correlation analysis showed that XPOT was positive related with cyclins and CDKs in TCGA datasets. Consistently, knockdown of XPOT down-regulated CDK1, CDK2, CDK4, CCNA1, CCNB1, CCNB2 and CCNE2 in HCC cells. XPOT can promote the cell cycle through up-regulating the cell cycle checkpoint. The results of GSEA also showed that XPOT was closely related with the gene sets in ubiquitin-mediated proteolysis. The ubiquitin-proteasome system (UPS) is a selective proteolytic system in which substrates are recognized and tagged with ubiquitin for processive degradation by the proteasome.<sup>21,22</sup> UPS is in charge of degrading 80-90% of proteins, which is central to regulating cellular function and maintaining protein homeostasis including cell cycle.<sup>23,24</sup> S-phase kinase-associated protein-1 (SKF-1)-cullin 1 (CUL1)-F-box protein (SCF) is the largest subfamily of E3 ligases regulating cell cycle progression at the G1/S transition.<sup>25</sup> SKP2 is well known as the F-box of the SCFskp2 ligase and was found to be an oncoprotein in HCC.<sup>26</sup> SKP2 can promote hepatoma cell proliferation through regulating cyclin A.<sup>27</sup> Cyclin A plays a prominent role in the initiation and completion of DNA replication during S-phase.<sup>28,29</sup> Thus, we concluded that XPOT may affect cell cycle transition through UPS in HCC.

In conclusion, we demonstrated that XPOT promotes tumor proliferation and invasion in HCC. Our results indicated that XPOT may affect the tumor cell cycle through ubiquitin-mediated proteolysis.

## ETHICS APPROVAL AND CONSENT TO PARTICIPATE

Informed consent was obtained from the patients or their family members who agreed to the use of their samples in this study.

## CONFLICT OF INTEREST

The authors declare that they have no competing interests.

## ORCID

Yuchen Hou  <http://orcid.org/0000-0003-2569-1680>

## REFERENCES

- Allemani C, Matsuda T, Di Carlo V, et al. Global surveillance of trends in cancer survival 2000–14 (CONCORD-3): analysis of individual records for 37 513 025 patients diagnosed with one of 18 cancers from 322 population-based registries in 71 countries. *Lancet*. 2018;391:1023–1075.
- Torre LA, Bray F, Siegel RL, Ferlay J, Lortet-Tieulent J, Jemal A. Global cancer statistics, 2012. *CA*. 2015;65:87–108.
- Fernandez-Sevilla E, Allard MA, Selten J, et al. Recurrence of hepatocellular carcinoma after liver transplantation: is there a place for resection? *Liver Transpl*. 2017;23:440–447.
- Forner A, Reig M, Bruix J. Hepatocellular carcinoma. *Lancet*. 2018;391:1301–1314.
- Wu L, Nguyen LH, Zhou K, et al. Precise let-7 expression levels balance organ regeneration against tumor suppression. *eLife*. 2015;4:e09431.
- Lee LH, Sadot E, Ivelja S, et al. ARID1A expression in early stage colorectal adenocarcinoma: an exploration of its prognostic significance. *Hum Pathol*. 2016;53:97–104.
- Lv J, Kong Y, Gao Z, Liu Y, Zhu P, Yu Z. LncRNA TUG1 interacting with miR-144 contributes to proliferation, migration and tumorigenesis through activating the JAK2/STAT3 pathway in hepatocellular carcinoma. *Int J Biochem Cell Biol*. 2018;101:19–28.
- Arts GJ, Fornerod M, Mattaj JW. Identification of a nuclear export receptor for tRNA. *Curr Biol*. 1998;8:305–314.
- Hellmuth K, Lau DM, Bischoff FR, Künzler M, Hurt E, Simos G. Yeast Los1p has properties of an exportin-like nucleocytoplasmic transport factor for tRNA. *Mol Cell Biol*. 1998;18:6374.
- Grosshans H, Hurt E, Simos G. An aminoacylation-dependent nuclear tRNA export pathway in yeast. *Genes Dev*. 2000;14:830–840.
- Melaiu O, Melissari E, Mutti L, et al. Expression status of candidate genes in mesothelioma tissues and cell lines. *Mutat Res*. 2015;771:6–12.
- Vaidyanathan S, Thangavelu PU, Duijff PH. Overexpression of ran GTPase components regulating nuclear export, but not mitotic spindle assembly, marks chromosome instability and poor prognosis in Breast cancer. *Target Oncol*. 2016;11:1–10.
- Suzuki T, Koyama Y, Hayakawa S, Munakata H, Isemura M. 1,25-Dihydroxyvitamin D3 suppresses exportin expression in human promyelocytic leukemia HL-60 cells. *Biomed Res*. 2006;27:89–92.
- Subramanian A, Tamayo P, Mootha VK, et al. Gene set enrichment analysis: a knowledge-based approach for interpreting genome-wide expression profiles. *Proc Natl Acad Sci U S A*. 2005;102:15545–15550.
- Cook AG, Fukuhara N, Jinek M, Conti E. Structures of the tRNA export factor in the nuclear and cytosolic states. *Nature*. 2009;461:60–65.
- Lund E, Guttinger S, Calado A, Dahlberg JE, Kutay U. Nuclear export of microRNA precursors. *Science*. 2004;303:95–98.

17. Lund E, Dahlberg JE. Proofreading and Aminoacylation of tRNAs before Export from the Nucleus. *Science*. 1998;282:2082–2085.
18. Hopper AK, Pai DA, Engelke DR. Cellular dynamics of tRNAs and their genes. *FEBS Lett*. 2010;584:310–317.
19. Leisegang MS, Martin R, Ramirez AS, Bohnsack MT. Exportin T and Exportin 5: tRNA and miRNA biogenesis – and beyond. *Biol Chem*. 2012;393:599–604.
20. Nuovo G, Tran H, Gutierrez A, et al. Importin-beta and exportin-5 are strong biomarkers of productive reoviral infection of cancer cells. *Ann Diagn Pathol*. 2018;32:28–34.
21. Ji CH, Kwon YT. Crosstalk and interplay between the ubiquitin-Proteasome system and autophagy. *Mol Cells*. 2017;40:441–449.
22. Crunkhorn S. Cancer: targeting the ubiquitin pathway. *Nat Rev Drug Discov*. 2018;17:166.
23. Tiwari I, Yoon MH, Park BJ, Jang KL. Hepatitis C virus core protein induces epithelial-mesenchymal transition in human hepatocytes by upregulating E12/E47 levels. *Cancer Lett*. 2015;362:131–138.
24. Chen YJ, Wu H, Shen XZ. The ubiquitin-proteasome system and its potential application in hepatocellular carcinoma therapy. *Cancer Lett*. 2015;379:245–252.
25. Bloom J, Cross FR. Multiple levels of cyclin specificity in cell-cycle control. *Nat Rev Mol Cell Biol*. 2007;8:149–160.
26. Calvisi DF, Ladu S, Pinna F, et al. SKP2 and CKS1 promote degradation of cell cycle regulators and are associated with hepatocellular carcinoma prognosis. *Gastroenterology*. 2009;137:1816–1826 e1811-1810.
27. Ji P, Goldin L, Ren H, et al. Skp2 contains a novel cyclin A binding domain that directly protects cyclin A from inhibition by p27Kip1. *J Biol Chem*. 2006;281:24058–24069.
28. Soucek T, Pusch O, Hengstschlägerottnad E, Adams PD, Hengstschläger M. Deregulated expression of E2F-1 induces cyclin A- and E-associated kinase activities independently from cell cycle position. *Oncogene*. 1997;14:2251–2257.
29. Pagano M, Pepperkok R, Verde F, Ansorge W, Draetta G. Cyclin A is required at two points in the human cell cycle. *Embo J*. 1992;11:961–971.

**How to cite this article:** Lin J, Hou Y, Huang S, et al. Exportin-T promotes tumor proliferation and invasion in hepatocellular carcinoma. *Molecular Carcinogenesis*. 2019;58:293–304. <https://doi.org/10.1002/mc.22928>